Optimal Control of Levitated Nanoparticles through Finite-Stiffness Confinement

Marco Baldovin,[1,2,*] Ines Ben Yedder,[3] Carlos A. Plata,[4] Damien Raynal,[3,5] Loïc Rondin,[3] Emmanuel Trizac,[2,6] and Antonio Prados[4]

[1]*Institute for Complex Systems, CNR, Università Sapienza, I-00185, Rome, Italy*
[2]*LPTMS, CNRS, Université Paris-Saclay, F-91405, Orsay, France*
[3]*CentraleSupélec, LuMIn, Université Paris-Saclay, ENS Paris-Saclay, CNRS, F-91405, Orsay, France*
[4]*Física Teórica, Multidisciplinary Unit for Energy Science, Universidad de Sevilla, Apartado de Correos 1065, E-41080, Sevilla, Spain*
[5]*Centre of Light for Life (CLL) and Institute for Photonics and Advanced Sensing (IPAS), The University of Adelaide, 5005, Adelaide, South Australia, Australia*
[6]*École Normale Supérieure de Lyon, F-69342, Lyon, France*

(Received 19 February 2025; accepted 25 July 2025; published 28 August 2025)

Optimal control of levitated nanoparticles subjected to thermal fluctuations is a challenging problem, both theoretically and experimentally. In this Letter, we compute the time-dependent harmonic confining potential that steers, in a prescribed time and with the minimum energetic cost, a Brownian particle between two assigned equilibrium states. We take full account of inertial effects, thus addressing the general underdamped dynamics, and, to address actual experimental conditions, the stiffness of the confining potential is required to be bounded. We carry out an experiment realizing the described protocol for an optically confined nanoparticle, which is shown to reach the target state within accuracy—while spending less energy than other protocols with the same duration, significantly shorter than the characteristic relaxation time. The results presented here are expected to have relevant applications in the design of optimal devices, such as engines at the nanoscale.

DOI: 10.1103/pss4-b69w

The field of optimal control aims at devising time-dependent protocols for the parameters controlling the dynamical evolution of a system, while minimizing a certain cost functional of its trajectory. This is relevant in a wealth of physical situations; specifically, we focus here on the control of nanodevices with stochastic dynamics. Therein, one is typically interested in minimizing the entropy production [1–7] or the connection time [8–13] between given initial and target states. In the lab, the controlled parameters are usually restricted to a certain finite region. For example, the stiffness κ of a harmonic trap is generally limited to a nonnegative range $\kappa_- \le \kappa \le \kappa_+$ [14], depending on the specific technique used to realize the harmonic potential. As a rule, these inequalities make variational calculus unreliable for solving the optimization problem: more sophisticated techniques from optimal control theory are necessary.

Despite recent advances in the control of colloidal particles [16,17], important aspects remain challenging. Notably, most of the theoretical [1,3,4,6,10,12,13,16,18–21] and experimental results [22,23] pertain to the overdamped regime, in which inertial effects are negligible. Therein, accelerating the connection between equilibrium states of a particle confined in an arbitrary potential has been shown to be feasible, by using several inverse engineering techniques [18,19,21] imported from the field of shortcuts to adiabaticity [24]. Also, optimal protocols that minimize certain figures of merit have been investigated, e.g., minimization of irreversible work (entropy production) for a given connection time t_f, both for unbounded [1,3,4,6] and bounded [20] stiffness.

Extending control of colloidal particles to the underdamped regime is critical, since it is the most general description. Experimentally, underdamped dynamics accurately describes nanomechanical resonators [25,26] or levitated particles in moderate vacuum [27–29]. Theoretically, the control problem is significantly more complex and more poorly understood than its overdamped counterpart. Inverse engineering techniques have been used but limitations appear [30]—and optimal control brings about new challenges. Optimal protocols, in general, involve nonconservative, velocity-dependent driving forces [5,19,31]. If the force is restricted to be conservative, as done in this Letter, the optimal driving involves Dirac-delta type discontinuities [2]—which are not realizable in the lab, since they involve infinite values of the stiffness.

Our main goal is the optimal control of an underdamped particle, bringing to bear the practical bounds to achieve the optimal realizable protocol. In particular, we aim at minimizing the irreversible contribution to the work for a harmonically confined particle, with stiffness κ that can be tuned at will in a certain finite interval $0 \le \kappa_- \le \kappa \le \kappa_+$. Both the initial and target states correspond to equilibrium,

*Contact author: marco.baldovin@cnr.it

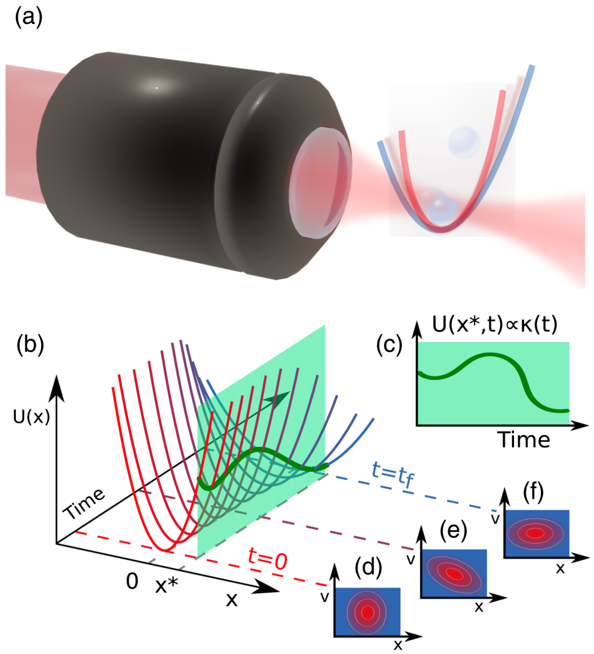

FIG. 1. Principle of the experiment. (a) A nanoparticle is optically levitated by a highly focused laser. The harmonic confinement of the particle, i.e., trap stiffness, is tuned through the trapping laser power. (b) The trap stiffness κ is changed in time according to a prescribed protocol (c), to bring the particle probability density function from an initial equilibrium state at time $t = 0$ (d) to a final equilibrium state at time $t = t_f$ (f), passing through a series of out-of-equilibrium states (e). The green section cutting plot (b) at an arbitrary $x = x^*$ provides a direct visualization of the time dependence of $\kappa(t)$. The connection can be achieved in a plethora of ways, and we seek for optimal ones (timewise or energywise).

for the initial and target values of the stiffness. It is worth stressing that the stiffness is the only parameter we control, i.e., the potential is harmonic, conservative, and confining at all times. Our theoretical results are tested by performing an experiment on a levitated nanoparticle trapped in an optical confining potential. The principle of the experiment, described below, is illustrated in Fig. 1.

Model—Consider a Brownian particle of mass m, position $\mathbf{x}$ and velocity $\mathbf{v}$, immersed in a fluid at constant temperature T. The collisions with the fluid molecules result in a damping force $-\gamma\mathbf{v}$, where γ is a constant friction coefficient, plus a fluctuating force $\boldsymbol{\xi}(t)$ such that $\langle\boldsymbol{\xi}(t)\rangle = 0$, $\langle\boldsymbol{\xi}(t)\boldsymbol{\xi}^T(t')\rangle = 2\gamma k_B T I\delta(t-t')$, where I represents the identity matrix and k_B is the Boltzmann constant. If the particle is trapped along a certain direction by the harmonic potential $U(x,t) = \kappa(t)x^2/2$, the projected motion obeys $\dot{x} = v$, $m\dot{v} = -\kappa x - \gamma v + \xi$. Equivalently, the probability density function $p(x,v,t)$ evolves through the Klein-Kramers equation [32],

$$\partial_t p = -\partial_x(vp) + \frac{1}{m}\partial_v\left(\kappa x p + \gamma v p + \frac{\gamma k_B T}{m}\partial_v p\right), \tag{1}$$

which admits the equilibrium solution for constant κ,

$$p_{\mathrm{eq}}(x,v|\kappa) = \frac{\sqrt{m\kappa}}{2\pi k_B T}\exp\left(-\frac{mv^2+\kappa x^2}{2k_B T}\right). \tag{2}$$

The above notation emphasizes that, in typical experimental setups, κ is a controllable parameter, while T is fixed. For an initial Gaussian centered at $(x = 0, v = 0)$, as in equilibrium, Eq. (1) preserves this property throughout the evolution of $p(x,v,t)$. The system's state is then completely characterized by the vector $\mathbf{u}$ of its second moments—see Sec. I of [33]. In terms of

$$u_1 = \frac{\gamma^2\langle x^2\rangle}{k_B T m}, \qquad u_2 = \frac{\gamma\langle xv\rangle}{k_B T}, \qquad u_3 = \frac{m\langle v^2\rangle}{k_B T}, \tag{3a}$$

$$s = \gamma t/m, \qquad k = m\kappa/\gamma^2, \tag{3b}$$

the evolution of the system's state reads

$$\dot{\mathbf{u}} = \mathbf{f}(\mathbf{u};k) \equiv M_k\mathbf{u} + 2\mathbf{e}_3, \tag{4}$$

in dimensionless variables, with $\dot{\mathbf{u}} \equiv d\mathbf{u}/ds$, and

$$M_k = \begin{pmatrix} 0 & 2 & 0 \\ -k & -1 & 1 \\ 0 & -2k & -2 \end{pmatrix}, \qquad \mathbf{e}_3 = \begin{pmatrix} 0 \\ 0 \\ 1 \end{pmatrix}. \tag{5}$$

We search for swift state-to-state transformations (SSTs) [16] between an initial state $p_{\mathrm{eq}}(x,v|\kappa_i)$ and a target equilibrium distribution $p_{\mathrm{eq}}(x,v|\kappa_f)$ corresponding to different confinements or, equivalently, between

$$\mathbf{u}_i = \begin{pmatrix} 1/k_i \\ 0 \\ 1 \end{pmatrix} \quad \text{and} \quad \mathbf{u}_f = \begin{pmatrix} 1/k_f \\ 0 \\ 1 \end{pmatrix}. \tag{6}$$

To do so, we allow $k(s)$ to vary with arbitrary speed, and even to make discontinuous jumps, but require it to remain within prescribed bounds, as follows:

$$0 \le k_- \le k \le k_+, \tag{7}$$

with $k_- < k_{i,f} < k_+$. We ask (i) whether the connection can be completed in a given finite time s_f by suitably steering k within the prescribed range (7), without waiting for the system's spontaneous relaxation; (ii) what SST protocol, from the plethora of them making the connection, minimizes the associated average external work. Since the cumulative average work at time s is

$$W(s) = k_B T \int_0^s ds' \frac{\dot{k}(s')}{2} u_1(s'), \tag{8}$$

we then look for the protocol $k(s)$ that minimizes $W(s_f)$.

The main tool for deriving our analytical results is Pontryagin's maximum principle (PMP) for minimizing a prescribed cost $\mathcal{C} = \int_0^{s_f} ds\, \mathcal{L}(\mathbf{u}; k)$ functional of the whole trajectory [34,35]. In a nutshell, PMP states that the time-dependent protocol $k(s)$ that minimizes $\mathcal{C}$ in turn maximizes the Hamiltonian $\mathcal{H}(\mathbf{u}, \boldsymbol{\varphi}; k) = \varphi_0 \mathcal{L}(\mathbf{u}; k) + \boldsymbol{\varphi} \cdot \mathbf{f}$, where $\varphi_0 \leq 0$ is a constant and $\boldsymbol{\varphi}$ is a vector of conjugated momenta, with $\mathbf{u}$ and $\boldsymbol{\varphi}$ obeying the canonical equations $\dot{\mathbf{u}} = \nabla_{\boldsymbol{\varphi}} \mathcal{H} = \mathbf{f}$ and $\dot{\boldsymbol{\varphi}} = -\nabla_{\mathbf{u}} \mathcal{H}$, with $(\varphi_0, \boldsymbol{\varphi}^T) \neq (0,0,0,0)$. Note that PMP provides a necessary, but in general not sufficient, condition for optimality. See Sec. II of [33] for more details.

Minimal time—To address our first question, we search for the minimum connection time s_{th} between $\mathbf{u}_i$ and $\mathbf{u}_f$. Here, $\mathcal{L} = 1$, and Pontryagin's Hamiltonian thus reads $\mathcal{H} = \varphi_0 + \boldsymbol{\varphi} \cdot \mathbf{f}(\mathbf{u}; k)$; its maximum can be located only at the extreme values $k = k_\pm$ [36]. Therefore, the minimum time is provided by a protocol alternating at least three branches with constant $k = k_\pm$, known as "bang-bang" in control theory [8,9,11,12,37–40]. The switching times and the total time s_{th} are numerically computed in Sec. III of [33]. If a protocol $k^\star(s)$ evolves $\mathbf{u}_i$ into $\mathbf{u}_f$ in a time s_{th}, the same connection can be made in any time $s_f > s_{\text{th}}$ [41]. Therefore, our first result is that $s_f \geq s_{\text{th}}$ is a sufficient condition to realize the desired connection.

Minimal work—Our next step is to search for the protocol that minimizes the total work among those achieving the connection in a time $s_f \geq s_{\text{th}}$. The total average work (8) splits into two contributions: (i) a reversible one, which is physically related to the free energy variation; and (ii) an irreversible one, which is a functional of $\mathbf{u}$ and k, vanishing in the quasistatic limit (see Sec. IV of [33]):

$$W_{\text{irr}} = k_B T \int_0^{s_f} ds \underbrace{\left(\frac{u_1}{u_1 u_3 - u_2^2} + u_3 - 2 \right)}_{P_{\text{irr}}}. \tag{9}$$

The optimal solution is found by minimizing either W_{irr} directly or the excess work with respect to the energy variation $\mathcal{C} = \int_0^{s_f} ds\,(u_3 - 1)$ [42]. Now $\mathcal{L} = u_3 - 1$ and, choosing $\varphi_0 = -1$, $\mathcal{H} = -u_3 + 1 + \boldsymbol{\varphi} \cdot \mathbf{f}(\mathbf{u}; k)$. The maximum of $\mathcal{H}$ as a function of k can be at either a value k_0 such that $\partial \mathcal{H}/\partial k|_{k=k_0} = 0$ or the bounds $k_\pm$. The first option yields, as shown in Sec. IV of [33],

$$\dot{k}_0 = 3k_0 + \frac{6}{u_1} + 3\frac{u_2}{u_1} - 9\frac{u_3}{u_1} + 10\frac{u_2^2}{u_1^2} - 8\frac{u_2 u_3}{u_1^2} + 8\frac{u_2^3}{u_1^3}, \tag{10}$$

which, if assumed to be valid $\forall\, s \in (0, s_f)$, leads to a protocol $k_0(s)$ that violates the bounds. In fact, this $k_0(s)$

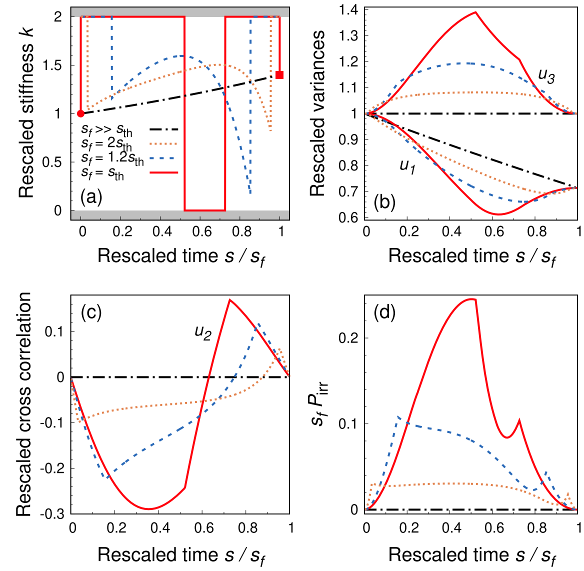

FIG. 2. Minimal work protocols. Panel (a) shows the optimal protocols for different values of the rescaled connection time s_f. The dash-dotted black curve corresponds to the quasistatic limit, $s_f \gg s_{\text{th}}$, while the solid red curve corresponds to the minimal-time protocol, $s_f = s_{\text{th}}$. Shaded areas denote forbidden values of the stiffness. In panels (b) and (c), the corresponding evolution of the rescaled moments u_1, u_2, and u_3 is shown. Finally, panel (d) exhibits the time dependence of the irreversible part of the average power [the integrand of Eq. (9)]. Plot axes are rescaled in such a way that the total area below each curve is proportional to the irreversible work done during each process, which decreases with t_f as expected. Here, $k_i = 1$, $k_f = 1.4$, $k_- = 0$, $k_+ = 2$.

coincides with the variational solution, which has Dirac-delta discontinuities at the initial and final times [43], and thus can be valid only for unbounded stiffness. Inspired by the structure of the unbounded solution, we look for a three-stage protocol in the bounded case:

$$k(s) = \begin{cases} k_\pm, & s \in [0, s_1], \quad \text{(bang)}, \\ k_0(s), & s \in [s_1, s_2], \quad \text{(Euler-Lagrange)}, \\ k_\pm, & s \in [s_2, s_f], \quad \text{(bang)}. \end{cases} \tag{11}$$

This three-stage optimal protocol, together with the corresponding time evolution of the correlations and the irreversible output power, is illustrated in Fig. 2.

Note that we expect a timescale separation between the (slow) control dynamics and the (fast) system thermalization for $s_f \to \infty$. Then, the optimal solution tends toward the overdamped limit one [5,44,45], namely,

$$k(s) = \left(\frac{s_f - s}{\sqrt{k_i} s_f} + \frac{s}{\sqrt{k_f} s_f} \right)^{-2}, \tag{12}$$

which can be realized without exceeding the range $k \in [k_i, k_f] \subset [k_-, k_+]$. We thus expect the optimal solution in the time interval $[s_1, s_2]$, determined by $k_0(s)$, to verify $k_- \leq k_0(s) \leq k_+$ if $s_f \gg s_{\rm th}$. A three-stage optimal solution of the "bang–Euler-Lagrange–bang" type, as proposed above, should thus always be possible under these conditions. If $s_f \gtrsim s_{\rm th}$, a more complex shape may be required: see Sec. V of [33] for an explicit example.

Experimental results—To experimentally test the derived optimal protocol, we use an optically levitated particle in moderate vacuum and at room temperature ($T_0 = 290$ K) [29]. An infrared laser is strongly focused by an objective to generate an optical tweezer trapping a 68 nm radius spherical silica particle in a harmonic potential of natural frequency $\Omega \approx 2\pi \times 100$ kHz. The trap stiffness $\kappa = m\Omega^2$, with the particle mass $m \approx 2.4 \times 10^{-18}$ kg, is directly proportional to the trapping laser power $P_{\rm las}$. The system damping is enforced via the gas pressure $p_{\rm gas}$ in the experiment chamber. Specifically, we use $p_{\rm gas} \approx 5$ hPa, corresponding to $\tau^{-1} = \gamma/m = 2\pi \times 4.4$ kHz $\ll \Omega$, which belongs in the underdamped regime—note that τ is the natural relaxation time. Using an ancillary laser, we record the particle dynamics $x(t)$.

As discussed earlier, a critical limitation of experimental realizations of thermodynamic protocols is that the control parameters are limited to a finite range. We control the trap stiffness through the trapping laser power using an acousto-optic modulator, which technically limits the ratio of available stiffnesses κ_+/κ_- to a factor of, typically, ten. Specifically, we have $\kappa_- = 0.29$ pN/μm ($\Omega_- = 2\pi \times 55$ kHz) and $\kappa_+ \approx 2.77$ pN/μm ($\Omega_+ = 2\pi \times 170$ kHz). We address decompression protocols with compression factor $\chi = \kappa_f/\kappa_i = 0.5$, choosing $\kappa_i = \kappa_+$.

Under these conditions, the minimal threshold time for a protocol is $t_{\rm th} \approx 7$ μs. We experimentally realize the derived SST optimal protocols for the minimization of the irreversible work [46]. They are shown in the inset of Fig. 3: the minimal-time protocol (violet) with a final time $t_f = t_{\rm th}$; an intermediate-time optimal protocol (red, $t_f = 1.8 t_{\rm th}$); and a long-time-limit protocol following Eq. (12) (orange, $t_f = 480$ μs $\gg t_{\rm th}$). As shown in Fig. 3, the resulting position variance $\langle x^2(t) \rangle$ reaches its final equilibrium value close to t_f, matching the theoretical expectation. Thus, the bounded optimal protocols successfully drive the system to equilibrium at the targeted final time. For the minimum time protocol, a small discrepancy between the experimental and theoretical processes is observed, which we attribute to the challenge of precisely matching experimental parameters: for $t_f = t_{\rm th}$, the duration of the bangs is close to the typical response time of the experimental setup.

For $t_f = t_{\rm th}$, there is only one protocol, the brachistochrone, that makes the connection at an expensive work cost; for $t_f \gg t_{\rm th}$, any regular protocol would be quasistatic and give a very small irreversible work, virtually indistinguishable from that for the optimal one given by Eq. (12). From the experimental point of view, the intermediate time, $t_f > t_{\rm th}$ with $t_f/t_{\rm th} = O(1)$, is thus the most interesting regime for our protocols with minimal work because it offers an advantageous trade-off between energetic cost and protocol duration. Therefore, we have considered two SST protocols with the same finite connection time $t_f = 1.8 t_{\rm th}$, shown in the inset of Fig. 4: the optimal one, given by Eq. (11), and a nonoptimal one. The latter relies on choosing the lowest-order polynomial that makes the connection [29,30]. For reference, we also consider a STEP protocol corresponding to a sudden change of stiffness from κ_i to κ_f.

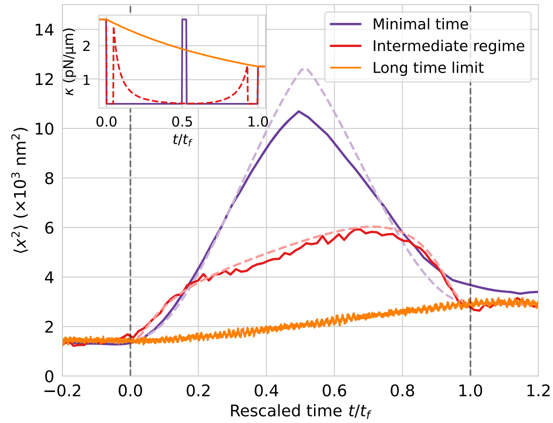

FIG. 3. Position variance for the experimental realization of optimal protocols. The plotted data correspond to 30 000 realizations of the minimal time (violet, $t_f = t_{\rm th} = 7$ μs), bounded optimal in the intermediate-time regime (red, $t_f = 1.8 t_{\rm th} = 12.6$ μs), and long-time-limit (orange, $t_f = 480$ μs $\gg t_{\rm th}$) protocols. All experiments correspond to the same bounds and compression factor of $\chi = 0.5$. The experimental variance evolutions fairly agree with analytical expectations (dashed lines). Vertical black dashed lines mark the initial and final times of the protocols, which are shown in the inset.

As previously, we look into the time evolution of the particle position variance driven by these protocols—bounded optimal, nonoptimal SST, and STEP—which is shown in Fig. 4(a). As expected, in the case of the STEP protocol, the variance presents oscillations with an exponential decay of characteristic time $\tau = m/\gamma \approx 3.8 \times 10^{-5}$ s, and it takes infinite time to exactly reach the target equilibrium state. In contrast, both the SST and the optimal protocol allow one to reach the target state at the desired final time $t_f = \tau/3 = 1.8 t_{\rm th}$.

We then compute the average experimental work required to drive the particle according to the three protocols using the definition (8) as detailed in Secs. VI and VII of [33]. The cumulative work resulting from the experimental measurements is shown in Fig. 4(b). At the final time t_f, we confirm that the bounded optimal protocol allows us to reach equilibrium with average work $W_{\rm optimal} = -0.19 k_B T$, lower than for the nonoptimal SST protocol under similar conditions, $W_{\rm SST} = -0.07 k_B T$. The STEP protocol provides an even lower work up to t_f,

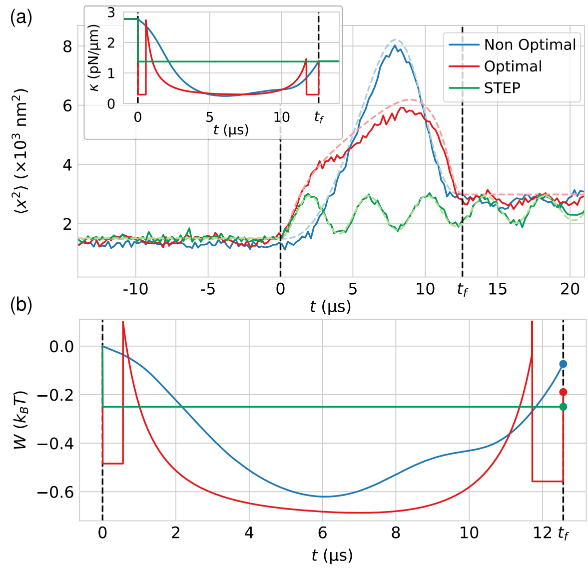

FIG. 4. (a) Position variance of the particles. The plotted data correspond to 30 000 realizations of STEP (green), nonoptimal SST (blue), and bounded optimal SST (red) protocols, whose associated stiffnesses are shown in the inset. The final time of both the nonoptimal SST and the bounded optimal SST is $t_f \approx 12.6$ μs. A fit of the STEP relaxation provides access to experimental parameters (red dashed line). The experimental data agree with analytical expectations (dashed lines). Vertical black dashed lines mark the starting and final times of the SST protocols. The optimal protocol is identical to the intermediate time regime protocol in Fig. 3 and is reproduced for clarity. (b) Experimental cumulative work performed for the STEP (green), nonoptimal SST (blue), and bounded optimal SST (red) protocols.

$W_{\mathrm{STEP}} = -k_B T/4$, but the system has not reached the target state.

Conclusions—The results shown in Fig. 4 account for a laboratory realization of the minimal-work transition between two equilibrium states of a levitated particle, subject to thermal noise and viscous friction, in a regime where inertial effects are relevant. The control protocol for the confining potential is applied within an actual experimental setup, showing that it can be implemented up to a very good degree of approximation. The target state is reached with the same accuracy as with the nonoptimized SST protocol studied in [29], but with a significantly lower energetic cost. The naive STEP protocol obtained by abruptly changing the confining stiffness and waiting for relaxation leads instead to a state that is far from being thermalized at the prescribed final time.

The present experiment puts forward a proof of principle for optimal control protocols at the nanoscale by showing that fast optimized transitions are realizable in the lab with levitated particles. Moreover, the results reported here are expected to be relevant, for instance, for the realization of thermal engines at scales where thermal effects are not negligible and stochastic thermodynamics must be taken into account [47–50]. Minimizing work done on the system—i.e., maximizing work extracted from it—at constant bath temperature is a typical building block in the design of efficient thermodynamic cycles: e.g., this corresponds to the optimal isothermal branches of maximum-power irreversible heat engines [51,52].

From the theoretical perspective, a challenging point to be further explored is the case of connection times close to the minimum time s_{th}. Therein, minimal work is usually not given by the three-stage process considered here (bang–Euler-Lagrange–bang), and more complex behaviors need to be taken into account. Also, we recall that PMP provides a necessary condition for optimality. Rigorously proving there is not any bounded SST protocol providing an even lower value for the considered cost functions, either connection time or irreversible work, is an open mathematical problem worthy of being investigated but beyond the scope of this Letter. Another research line concerns the more general case of nonharmonic confinements, which has recently been theoretically discussed [45,53], but in the limit of small inertial effects with unbounded stiffness. Finally, an interesting field of investigation involves the extension of control techniques to active-matter systems [54,55], for which some theoretical results are already available [56,57].

Acknowledgments—M. B. thankfully acknowledges useful discussions with J. Sanders and P. Muratore-Ginanneschi. M. B. was supported by ERC Advanced Grant RG.BIO (Contract No. 785932). C. A. P. and A. P. acknowledge financial support from Grant No. PID2024-155268NB-I00 funded by MICIU/AEI/10.13039/501100011033/ FEDER, UE, and also from the applied research and innovation Project No. PPIT2024-31833, cofunded by EU–Ministerio de Hacienda y Función Pública–Fondos Europeos–Junta de Andalucía–Consejería de Universidad, Investigación e Innovación. C. A. P., A. P., and E. T. acknowledge financial support from Grant ProyExcel_00796 funded by Junta de Andalucía's PAIDI 2020 program. C. A. P. acknowledges the funding received from the European Union's Horizon Europe-Marie Skłodowska-Curie 2021 program through the Postdoctoral Fellowship with Reference No. 101065902 (ORION). This work is supported by the ANR projects OPLA (ANR-20-CE30-0014) and FENNEC (ANR-23-CE30-0042).

Data availability—The data that support the findings of this article are openly available [46].

[1] T. Schmiedl and U. Seifert, Optimal finite-time processes in stochastic thermodynamics, Phys. Rev. Lett. **98**, 108301 (2007).

[2] A. Gomez-Marin, T. Schmiedl, and U. Seifert, Optimal protocols for minimal work processes in underdamped

stochastic thermodynamics, J. Chem. Phys. **129**, 024114 (2008).

[3] E. Aurell, C. Mejía-Monasterio, and P. Muratore-Ginanneschi, Optimal protocols and optimal transport in stochastic thermodynamics, Phys. Rev. Lett. **106**, 250601 (2011).

[4] E. Aurell, K. Gawedzki, C. Mejia-Monasterio, R. Mohayaee, and P. Muratore-Ginanneschi, Refined second law of thermodynamics for fast random processes, J. Stat. Phys. **147**, 487 (2012).

[5] P. Muratore-Ginanneschi, On extremals of the entropy production by 'Langevin-Kramers' dynamics, J. Stat. Mech. (2014) P05013.

[6] Y. Zhang, Work needed to drive a thermodynamic system between two distributions, Europhys. Lett. **128**, 30002 (2020).

[7] S. A. M. Loos, S. Monter, F. Ginot, and C. Bechinger, Universal symmetry of optimal control at the microscale, Phys. Rev. X **14**, 021032 (2024).

[8] G. C. Hegerfeldt, Driving at the quantum speed limit: Optimal control of a two-level system, Phys. Rev. Lett. **111**, 260501 (2013).

[9] G. C. Hegerfeldt, High-speed driving of a two-level system, Phys. Rev. A **90**, 032110 (2014).

[10] C. A. Plata, D. Guéry-Odelin, E. Trizac, and A. Prados, Finite-time adiabatic processes: Derivation and speed limit, Phys. Rev. E **101**, 032129 (2020).

[11] A. Prados, Optimizing the relaxation route with optimal control, Phys. Rev. Res. **3**, 023128 (2021).

[12] A. Patrón, A. Prados, and C. A. Plata, Thermal brachistochrone for harmonically confined Brownian particles, Eur. Phys. J. Plus **137**, 1011 (2022).

[13] A. Patrón, C. A. Plata, and A. Prados, Minimum time connection between non-equilibrium steady states: The Brownian gyrator, J. Phys. A **57**, 495004 (2024).

[14] Negative values of the stiffness are difficult to implement in the lab, although they have been realized employing feedback techniques [15].

[15] J. A. C. Albay, P.-Y. Lai, and Y. Jun, Realization of finite-rate isothermal compression and expansion using optical feedback trap, Appl. Phys. Lett. **116**, 103706 (2020).

[16] D. Guéry-Odelin, C. Jarzynski, C. A. Plata, A. Prados, and E. Trizac, Driving rapidly while remaining in control: Classical shortcuts from Hamiltonian to stochastic dynamics, Rep. Prog. Phys. **86**, 035902 (2023).

[17] S. Blaber and D. A. Sivak, Optimal control in stochastic thermodynamics, J. Phys. Comm. **7**, 033001 (2023).

[18] I. A. Martínez, A. Petrosyan, D. Guéry-Odelin, E. Trizac, and S. Ciliberto, Engineered swift equilibration of a Brownian particle, Nat. Phys. **12**, 843 (2016).

[19] G. Li, H. T. Quan, and Z. C. Tu, Shortcuts to isothermality and nonequilibrium work relations, Phys. Rev. E **96**, 012144 (2017).

[20] C. A. Plata, D. Guéry-Odelin, E. Trizac, and A. Prados, Optimal work in a harmonic trap with bounded stiffness, Phys. Rev. E **99**, 012140 (2019).

[21] C. A. Plata, A. Prados, E. Trizac, and D. Guéry-Odelin, Taming the time evolution in overdamped systems: Shortcuts elaborated from fast-forward and time-reversed protocols, Phys. Rev. Lett. **127**, 190605 (2021).

[22] S. Ciliberto, Experiments in stochastic thermodynamics: Short history and perspectives, Phys. Rev. X **7**, 021051 (2017).

[23] I. A. Martínez, E. Roldán, L. Dinis, and R. A. Rica, Colloidal heat engines: A review, Soft Matter **13**, 22 (2017).

[24] D. Guéry-Odelin, A. Ruschhaupt, A. Kiely, E. Torrontegui, S. Martínez-Garaot, and J. G. Muga, Shortcuts to adiabaticity: Concepts, methods, and applications, Rev. Mod. Phys. **91**, 045001 (2019).

[25] A. Le Cunuder, I. A. Martínez, A. Petrosyan, D. Guéry-Odelin, E. Trizac, and S. Ciliberto, Fast equilibrium switch of a micro mechanical oscillator, Appl. Phys. Lett. **109**, 113502 (2016).

[26] S. Dago and L. Bellon, Dynamics of information erasure and extension of Landauer's bound to fast processes, Phys. Rev. Lett. **128**, 070604 (2022).

[27] L. Rondin, J. Gieseler, F. Ricci, R. Quidant, C. Dellago, and L. Novotny, Direct measurement of Kramers turnover with a levitated nanoparticle, Nat. Nanotechnol. **12**, 1130 (2017).

[28] M. Rademacher, M. Konopik, M. Debiossac, D. Grass, E. Lutz, and N. Kiesel, Nonequilibrium control of thermal and mechanical changes in a levitated system, Phys. Rev. Lett. **128**, 070601 (2022).

[29] D. Raynal, T. De Guillebon, D. Guéry-Odelin, E. Trizac, J.-S. Lauret, and L. Rondin, Shortcuts to equilibrium with a levitated particle in the underdamped regime, Phys. Rev. Lett. **131**, 087101 (2023).

[30] M. Chupeau, S. Ciliberto, D. Guéry-Odelin, and E. Trizac, Engineered swift equilibration for Brownian objects: From underdamped to overdamped dynamics, New J. Phys. **20**, 075003 (2018).

[31] G. Li, J.-F. Chen, C. Sun, and H. Dong, Geodesic path for the minimal energy cost in shortcuts to isothermality, Phys. Rev. Lett. **128**, 230603 (2022).

[32] C. Gardiner, *Stochastic Methods: A Handbook for the Natural and Social Sciences*, Springer Series in Synergetics (Springer, Berlin—Heidelberg, 2009).

[33] See the Supplemental Material at http://link.aps.org/supplemental/10.1103/pss4-b69w for a concise summary of the main concepts of Pontryagin's theory, a full derivation of the optimal protocols, and a justification of our cost function. We also discuss a case with s_f close to $s_{\rm th}$, where our results cannot be straightforwardly applied and further analysis is needed. Finally, we provide further information on the experiment, explaining the calibration process and the method we use to compute the work.

[34] L. S. Pontryagin, *Mathematical Theory of Optimal Processes* (CRC Press, Boca Raton, 1987).

[35] D. Liberzon, *Calculus of Variations and Optimal Control Theory: A Concise Introduction* (Princeton University Press, Princeton and Oxford, 2012).

[36] Imposing $(\partial H/\partial k) = 0$ does not give a solution; see Sec. III of [33] for details.

[37] X. Chen, A. Ruschhaupt, S. Schmidt, A. del Campo, D. Guéry-Odelin, and J. G. Muga, Fast optimal frictionless atom cooling in harmonic traps: Shortcut to adiabaticity, Phys. Rev. Lett. **104**, 063002 (2010).

[38] X.-J. Lu, X. Chen, J. Alonso, and J. G. Muga, Fast transitionless expansions of Gaussian anharmonic traps

for cold atoms: Bang-singular-bang control, Phys. Rev. A **89**, 023627 (2014).

[39] Y. Ding, T.-Y. Huang, K. Paul, M. Hao, and X. Chen, Smooth bang-bang shortcuts to adiabaticity for atomic transport in a moving harmonic trap, Phys. Rev. A **101**, 063410 (2020).

[40] N. Ruiz-Pino and A. Prados, Optimal control of uniformly heated granular fluids in linear response, Entropy **24**, 131 (2022).

[41] E.g., by getting to $\mathbf{u}_f$ in a time $s_{\rm th}$ by applying $k^\star(s)$ and then keeping the system at equilibrium for a time $s_f - s_{\rm th}$ by setting $k(s) = k_f$.

[42] The two approaches are equivalent, because the boundary conditions are fixed: we pursue the latter, which is slightly easier; see Sec. IV of [33].

[43] Similarly to the situation found in Ref. [2], although the boundary conditions are different—see Sec. IV of [33] for details.

[44] P. Muratore-Ginanneschi and K. Schwieger, How nanomechanical systems can minimize dissipation, Phys. Rev. E **90**, 060102(R) (2014).

[45] J. Sanders, M. Baldovin, and P. Muratore-Ginanneschi, Optimal control of underdamped systems: An analytic approach, J. Stat. Phys. **191**, 117 (2024).

[46] M. Baldovin, I. B. Yedder, C. A. Plata, D. Raynal, L. Rondin, E. Trizac, and A. Prados, Supporting data for “Optimal control of levitated nanoparticles through finite-stiffness confinement”, Zenodo repository, 10.5281/zenodo.13143005 (2025).

[47] A. Dechant, N. Kiesel, and E. Lutz, All-optical nanomechanical heat engine, Phys. Rev. Lett. **114**, 183602 (2015).

[48] C. Li, S. Zhu, P. He, Y. Wang, Y. Zheng, K. Zhang, X. Gao, Y. Dong, and H. Hu, Realization of an all-optical underdamped stochastic Stirling engine, Phys. Rev. A **109**, L021502 (2024).

[49] M. Message, F. Cerisola, J. D. Pritchett, K. O’Flynn, Y. Ren, M. Rashid, J. Anders, and J. Millen, Extreme-temperature single-particle heat engine, arXiv:2501.03677.

[50] M. Chatterjee, V. Holubec, and R. Marathe, Optimal constrained control for generally damped Brownian heat engines, J. Phys. A **58**, 245001 (2025).

[51] C. A. Plata, D. Guéry-Odelin, E. Trizac, and A. Prados, Building an irreversible Carnot-like heat engine with an overdamped harmonic oscillator, J. Stat. Mech. (2020) 093207.

[52] I. Prieto-Rodríguez, A. Prados, and C. A. Plata, Maximum-power stirling-like heat engine with a harmonically confined Brownian particle, Entropy **27**, 72 (2025).

[53] J. Sanders, M. Baldovin, and P. Muratore-Ginanneschi, Minimal work protocols for inertial particles in nonharmonic traps, Phys. Rev. E **111**, 034127 (2025).

[54] S. Shankar, V. Raju, and L. Mahadevan, Optimal transport and control of active drops, Proc. Natl. Acad. Sci. U.S.A. **119**, e2121985119 (2022).

[55] H. Massana-Cid, C. Maggi, G. Frangipane, and R. Di Leonardo, Rectification and confinement of photokinetic bacteria in an optical feedback loop, Nat. Commun. **13**, 2740 (2022).

[56] M. Baldovin, D. Guéry-Odelin, and E. Trizac, Control of active Brownian particles: An exact solution, Phys. Rev. Lett. **131**, 118302 (2023).

[57] L. K. Davis, K. Proesmans, and E. Fodor, Active matter under control: Insights from response theory, Phys. Rev. X **14**, 011012 (2024).